Journal of Cellular Biochemistry 102:955–969 (2007)

# The Murine Ortholog of the SHP-2 Binding Molecule, PZR Accelerates Cell Migration on Fibronectin and Is Expressed in Early Embryo Formation

**Maria G. Roubelakis,[1,2,3]* Enca Martin-Rendon,[1] Grigorios Tsaknakis,[1,2] Athanassios Stavropoulos,[4] and Suzanne M. Watt[1,2]**

[1]Stem Cell Research Laboratory, National Blood Service, NHS Blood and Transplant Authority, Oxford OX3 5BG, UK
[2]Nuffield Department of Clinical Laboratory Sciences, University of Oxford, Oxford OX3 5BG, UK
[3]Cell and Gene Therapy Laboratory, Centre of Basic Research, Foundation for Biomedical Research of the Academy of Athens (IIBEAA), Athens 11527, Greece
[4]Centre of Transplantation and Immunology, Foundation for Biomedical Research of the Academy of Athens (IIBEAA), Athens 11527, Greece

**Abstract** The human P zero-related protein (hPZR) has a unique function in regulating cell migration. This activity is dependent on both its cytoplasmic immunoreceptor tyrosine inhibitory motif (ITIM) and its interaction with the tyrosine protein phosphatase, src homology phosphatase-2 (SHP-2). Here, using in silico and cDNA cloning approaches, we identify the murine ITIM-containing hPZR ortholog, mPZR, together with its ITIM-less isoform, mPZRb. We demonstrate that, like hPZR, these type 1 integral murine transmembrane isoforms are derived by differential splicing from a single gene transcription unit on mouse chromosome 1, and differ only in the sequence of their cytoplasmic domains. Importantly, mPZR mimicks hPZR functionally by accelerating SHP-2-mediated cell migration on fibronectin. Interestingly, we further demonstrate that although neither mPZR nor mPZRb is expressed in murine pluripotent embryonic stem cells, they first appear at approximately day 3 of blastocyst formation in vivo and of embryoid body formation in vitro. These studies thus provide the basis for defining the function of the mPZR isoforms in vivo, particularly with respect to their roles in regulating SHP-2-dependent cell migration during development. J. Cell. Biochem. 102: 955–969, 2007. 

**Key words:** PZR; SHP-2; ITIMs; tyrosine phosphatase; genomic structure; migration; embryonic stem cells

The src homology phosphatase-2 (SHP-2) signal transduction protein plays a critical role in controlling cell migration, and in regulating the balance between self-renewal, pluripotency and differentiation of murine (m) embryonic stem cells [Saxton et al., 1997; Qu et al., 1998; Chan et al., 2003]. It is ubiquitously expressed and highly conserved between species, containing two unique N-terminal SH2 domains, followed by a phosphatase domain (reviewed by Neel et al. [2003]). Mutations in the human (h) SHP-2 gene give rise to hematopoietic, cardiac, and skeletal disorders, resulting in Noonan and Leopard syndromes and some leukemias [Tartaglia et al., 2001; Neel et al., 2003; Tartaglia et al., 2004]. The importance of the N-terminal SH2 domain of SHP-2 is exemplified in mice or murine cell lines carrying the mutation, SHP-2 $\Delta^{46-116}$, where a 65 amino acid deletion in the N-terminal SH2 domain occurs. Murine SHP-2 $\Delta^{46-116}$ embryonic fibroblasts show defects in cell migration and spreading, and display an increased number of focal adhesions in vitro [Zannettino et al., 2003]. The same homozygous SHP-2 mutation is embryonic lethal in mice [Saxton et al., 1997]. However, chimeric mice derived from SHP-2

Grant sponsor: Leukaemia Research Fund; Grant sponsor: Medical Research Council; Grant sponsor: NHS Blood and Transplant Authority.

*Correspondence to: Maria G. Roubelakis, DPhil, Cell and Gene Therapy Laboratory, Centre of Basic Research, Foundation for Biomedical Research of the Academy of Athens, 4, Soranou Efesiou St., 11527 Athens, Greece.
E-mail: mroubelaki@bioacademy.gr

Received 9 June 2006; Accepted 13 February 2007
DOI 10.1002/jcb.21334

$\Delta^{46-116}$ heterozygous and homozygous mutant murine embryonic stem cell (mES) lines show skeletal, hematopoietic and vascular abnormalities, that are reminiscent of the human disorders described above [Qu et al., 1998].

The identification of interacting partners that modulate SHP-2 activity is of fundamental importance in defining its function. Some of those that have been defined include cytokine receptors, such as the c-kit tyrosine kinase receptor and the common gp130 subunit of the leukemia inhibitory factor (LIF) and oncostatin M receptors [Burdon et al., 2002]. More recently, we and others have identified the human P zero-related protein (hPZR) molecule as a SHP-2 binding partner with a novel function in modulating cell migration on fibronectin [Zhao and Zhao, 2000; Zhao et al., 2002, 2003; Zannettino et al., 2003]. This 43 kD transmembrane protein is composed of a single extracellular immunoglobulin (Ig) domain, a transmembrane (TM) region, and an 80 amino acid cytoplasmic domain. The latter contains two intracellular Ig immunoreceptor tyrosine-based inhibitory motifs (ITIMs) [Zhao et al., 2002; Zannettino et al., 2003]. These ITIMs are essential for the recruitment of phosphorylated SHP-2 and, subsequently, for activation of the SHP-2 protein phosphatase.

To begin to address the functional role of mPZR isoforms in vivo, we have cloned the ITIM-containing murine ortholog of hPZR, mPZR, and its ITIM-less isoform, mPZRb. The presence of the third hPZRa isoform was not detected in the mouse cells and tissues examined. We show that the mPZR protein, like its human counterpart, interacts with mSHP-2 and accelerates cell migration on fibronectin. Furthermore, we demonstrate that while mSHP-2 is expressed in murine self-renewing mES cells, mPZR and mPZRb are not, but appear initially by day 3 of embryoid body (EB) formation in vitro and at blastocyst stage in vivo. Our studies, thus provide the potential for future and more extensive functional studies on the relative roles of mPZR and mPZRb in vivo.

## MATERIALS AND METHODS

### Cell Lines

The murine fibroblastoid NIH3T3, monocytic/macrophage P388D1, pre-T EL4 and erythroid progenitor MEL-585 cell lines were obtained from American Type Cell Collection (ATCC, Manassas, VA) or European Collection of Cell Cultures (ECACC, Porton Down, Wiltshire, UK). All were maintained in Dulbecco's modified Eagle's medium (DMEM; Sigma–Aldrich Ltd, Gillingham, Dorset, UK) supplemented with 10% (v/v) fetal calf serum (FCS) (Gibco-BRL, Paisley, Scotland, UK). The murine multipotential progenitor cell line, FDCP-mix A4, was maintained in Fisher's Medium (Gibco-BRL), with 20% (v/v) horse serum and 2% (v/v) mIL3 conditioned medium (both kindly provided by Dr. Claire Heyworth, Patterson Institute of Cancer Research, Manchester, UK) [Heyworth et al., 1995].

### Antibodies and Flow Cytometry

The anti-Flag-epitope monoclonal antibody (Mab), M2 (Sigma–Aldrich), and the mouse anti-human WM78 monoclonal antibody to the PZR and PZRb extracellular domains together with fluorescein isothiocyanate (FITC) or phycoeryhrin (PE)-conjugated rabbit anti-mouse IgG secondary antibody (DakoCytomation, Glostrop, Denmark) were used for single or dual color flow cytometric analysis. As a negative isotype matched control, the mIgG1 Mab was used. Cells were analyzed on a FACStar$^{PLUS}$ flow cytometer using the CellQuest software (both from Becton-Dickinson, Sunnyvale, CA) [Watt et al., 2000]. The rabbit anti-SHP-2 polyclonal antibody and the irrelevant rabbit Ig control were purchased from Cell Signaling Technology, Inc., Beverly, MA.

### In Silico Cloning

cDNA and genomic cloning of murine PZR and PZRb. hPZR cDNA was prepared and its genomic structure determined as described previously [Zannettino et al., 2003]. The mPZR cDNA (GenBank accession number: **AY764247**) and genomic sequences were identified by in silico cloning (NCBI, Genebank, Blast Server, http://www.ncbi.nlm.nih.gov and ENSEMBL, http://www.ensembl.org/) using the hPZR nucleotide sequence as the query sequence. The cDNA sequences were confirmed by RT-PCR (reverse transcriptase–polymerase chain reaction) analyses using RNAs extracted from a variety of cell lines. Total RNAs were isolated from approximately $10^6$–$10^7$ cells using the RNeasy RNA isolation kit (Qiagen Ltd, Crawley, West Sussex, UK) and reverse transcribed using the Sensiscript Reverse Transcriptase

system (Qiagen Ltd). PCR amplification was carried out on the cDNAs using the Thermostart DNA polymerase and reagents (Abgene, Inc., Rochester, NY) plus the mPZR forward (F) and reverse (R) primer pairs: (mPZR F1, forward primer: 5′-T C A G G C T G T T C A C A A T G G C A C C-′3 and mPZR R1, reverse primer: 5′-G G A C C A C G G G A T G C T T C T A A A A C-′3). The forward (F) and reverse (R) primer pair for PCR amplification of the mPZRa isoform, similarly to the human, was (mPZRa F, forward primer: 5′-A G C C T C T T C C C C A A G C C G A G-′3 and mPZRa R, reverse primer: 5′-C C C T G C C C T A A A A A A A C A G-′3). The TMHMM V2 prediction server (http://www.cbs.dtu.dk/services.TMHMM) was used for prediction of transmembrane helices in proteins and predicted structures and motifs were determined according to Zannettino et al. [2003]. The NetNGlyc 1.0 Prediction server (http://www.cbs.dtu.dk/services/NetNGlyc/) was also used for the prediction of N-linked glycosylation sites.

### Growth and Differentiation In Vitro of mES Cells

The mES cell line, E14, was routinely maintained in an undifferentiated state on tissue culture grade plates coated with gelatin (0.1% (w/v); Sigma–Aldrich) in DMEM-ES medium (Gibco-BRL) containing 1% (v/v) non-essential amino acids, 0.007% (v/v) 2-mercaptoethanol, $10^4$ U/ml LIF (Esgro Chemicon Int., Temecula, CA) and 15% (v/v) prescreened FCS (Stem Cell Technologies, Vancouver, Canada) [Keller et al., 1993]. Twenty-four to 48 h prior to differentiation, the mES cells were transferred into Iscove's modified Dulbecco's-ES medium (IMDM-ES) (Gibco-BRL) supplemented with $10^4$ U/ml LIF and 15% (v/v) pre-screened FCS. In order to generate EBs, mES cells were trypsinized, and 3,000–5,000 cells were plated onto the bacterial grade plates without gelatin coating, and then cultured in IMDM-ES differentiation medium with 15% (v/v) FCS, 2 mM L-glutamine, 5% (v/v) protein free hybridoma medium (PFHM-II; Gibco-BRL), $4 \times 10^4$ U/ml monothioglycerol and 50 μg/ml ascorbic acid (both from Sigma–Aldrich), but in the absence of LIF. The developing EBs were maintained at 37°C in a 5% (v/v) humidified $CO_2$ incubator for up to 6 days [Keller et al., 1993, 1999; Keller, 1995]. The mES cells and developing EBs were viewed under a T-300 Nikon inverted microscope fitted with DIC and Hoffman optics (Nikon Ltd, Kingston, Surrey, UK) and images were recorded with an Orca AG fire wire Camera and the IPLab software package (both from Nikon Ltd).

### RNA Extraction and RT-PCR Analysis of Cells, Embryoid Bodies and Tissues

RNAs from cell lines, EBs, or tissues were extracted with Trizol (Gibco-BRL). cDNAs were reverse transcribed from 1 μg of RNA using the MMLV reverse transcriptase enzyme and kit (Promega Ltd, Madison, WI) according to the manufacturer's instructions and with 30–60 cycles of PCR. The cDNAs were analyzed on agarose gels, and extracted and sequenced as described [Chan et al., 2001]. cDNAs for mouse adult tissues and mouse days 11, 15, and 17 embryos were obtained from Clontech (Clontech Laboratories, Inc., Palo Alto, CA). The following primer pairs were used for PCR amplification: mOCT-4 F: G G C G T T C T C T T T G G A A A G G T G T T C; mOCT-4 R: C T C G A A C C A C A T C C T T C T C T; mBRACHYURY F: T G C T G C C T G T G A G T C A T A A C; mBRACHYURY R: T C C A G G T G C T A T A T A T A T T G C C; mBMP-4 F: A C T G T G A G G A G T T T C C A T C A G G; mBMP-4 R: T C T T A T T C T T C T T C C T G G A C C G; mFLK-1 F: T A G G T G C C T C C C C A T A C C C T G G; mFLK-1 R: TGGCCGGCTCTTTCGCTTACTG; mSHP-2 F: C T C A A G C A G C C C C T C A A C A C A A; mSHP-2 R: G A A C A C C A T C C G C C A G A A G T C A T (Sigma Genosys Ltd, Haverhill, UK); mGAPDH forward and reverse primers from Clontech Laboratories, Inc.

### Real Time Quantitative PCR

The reaction and analysis were performed as described by Zannettino et al. [2003]. The mPZR and mPZRb TaqMan™ systems (Applied Biosystems, Foster City, CA) consist of the following pair of primers: F mPZR 5′-T T A A G C A G G C T C C A C G G A A G T-3′, R mPZR 5′-C A T T T A C G C A C A G T T A G A C C A C T C T -3′ and F mPZRb 5′-A G G A A A C A T T C G A A G C G G G A T T-3′, R mPZRb 5′-A C A A G T C A G A G T C T G T G G T G T A T G C-3′, respectively, as well as dual fluorescent probes mPZR (5′-C C C T C C G A C A C A G A G G G T C T A G T A A A G A G T C-3′) and mPZRb (5′-A C C G G G G C C C A G T C A T T T A C G C A C A G T T-3′). The level of expression of mPZR and mPZRb isoforms was normalized after subtracting the Ct value of

the mGAPDH internal control (GAPDH, TaqMan® pre-developed assay reagents, Applied Biosystems No. 4352932E) from that of Ct value for mPZR or mPZRb ($\Delta Ct = |Ct_{mPZR \text{ or } mPZRb} - Ct_{GAPDH}|$) for each tissue analyzed. Then, the relative level of mPZR was compared to mPZRb by setting the mPZRb value to 1 for each individual tissue and determining the fold change in expression of mPZR against this value using the formula $2^{\Delta Ct}$. In order to compare the levels of mPZR expression between tissues, the $\Delta\Delta Ct$ value for each tissue was determined using the formula ($\Delta\Delta Ct = \Delta Ct_{mPZR} - \Delta Ct_{mPZR \text{ from the lowest expressing tissue}}$), the fold difference calculated and each resulting value normalized against the highest level of expression, which occurred in the E17 embryonic tissue and which was set to 100%.

### Embryo Recovery

C57bl/6 female mice (3–4 weeks old) (Charles River Laboratories, Inc., Wilmington, MA) were given free access to food and water and were maintained on a 12L:12D photoperiod. These female mice were superovulated by injecting 5 international units of gonadotropin from pregnant mare serum (PMS) (Sigma–Aldrich), followed by 5 international units of human (h) chorionic gonadotropin (hCG) (Sigma–Aldrich) 48 h later. Females were mated with C57bl/6 males of proven fertility overnight following the hCG injection. Mating was confirmed by identification of a vaginal plug. For the timing of the embryo collection, the morning of the day of the vaginal plug identification was taken as E0.5. Mated females were sacrificed 48 and 96 h post-hCG injection (embryonic day (E) 1.5 and 3.5) to recover embryos at the two cells and blastocyst stages by flushing oviducts and uterine horns respectively in M1 medium (Sigma–Aldrich). The E12.5 embryos were removed from the uterus in phosphate buffer saline (pH7.2). All procedures described above were reviewed and approved by the animal studies committee of the local authority and were performed in accordance with Institutional Animal Care and Use Committee approval.

### Immunofluorescent Staining

E1.5 and E3.5 old embryos were washed in PBS solution and incubated in 1 ml Tyrode's solution (Sigma–Aldrich) for 30 s to remove the zona pellucidae. The embryos were then placed on glass slides treated with poly-L-lysine (Sigma–Aldrich), fixed in 2% (w/v) paraformaldehyde (Sigma–Aldrich) for 1 h and permeabilized in PBS solution containing 0.1% (v/v) Triton X-100 (Sigma–Aldrich) for 30 min. Slides were then incubated in the blocking solution (Mouse on Mouse (MOM) Ig Blocking reagent, Vector MOM Immunodetection Kit, Vector laboratories, Inc., CA] for 1 h, followed by PBS washing and a 5 min incubation in MOM diluent solution (Vector laboratories, Inc.). Fifty μl of 1.5μg/ml WM78 primary antibody or isotype specific control were added to each slide for an overnight incubation. After extended washes in 0.1% (v/v) Triton X-100 PBS, Alexa 488-conjugated goat-anti mouse IgG1 secondary antibody (Molecular Probes) was added to the slides in MOM diluent solution for 30 min. Slides underwent additional washes in 0.1% (v/v) Triton X-100 PBS and mounted with Vectashield mounting medium (Vector laboratories, Inc.) containing DAPI solution. All incubations were carried out at 4°C unless stated otherwise. The controls included blocking solution without primary antibody, nonimmune rabbit IgG (500 ng/ml) (Sigma–Aldrich), blocking solution with secondary antibody and untreated embryos. Images were acquired using an automated Leica TCS SP5 confocal microscope fitted with HeNe 543, HeNe 633 and argon 488 lasers.

### Sectioning and Peroxidase Immuno-Staining

E12.5 old murine embryos were embedded in paraffin, cut into 5 μm sagital sections and then mounted onto slides. The slides were deparaffinizated in xylene followed by washes in 100%, 90%, and 70% (v/v) ethanol, respectively. The slides were post fixed in 2% (w/v) paraformaldehyde (Sigma–Aldrich) for 10 min. Antigen was retrieved with 10 mM sodium citrate (Sigma–Aldrich) for 30 min at 80°C. The WM78 Mab or isotype specific control was diluted in MOM™ diluent (Vector laboratories, Inc., CA) and used at 1.5 μg/ml. The staining was performed using the Vector® MOM™ Peroxidase kit (Vector laboratories, Inc., CA) according manufacturer's instructions.

### Production and Transient Transfection of mPZR and mPZRb

The mPZR-flag and mPZRb-flag constructs containing the *FLAG* epitope at the 5′ end was generated using the following primer pairs: mPZR F2 (for both constructs): C C G C T C G A

GCGGATGGACTACAGGACGATGAC AAGGCAGAGGCCGTCGGAGCC and mPZR R2: CCGGAATTCCGGTCAGTCT TTCCGGATGTCCGCATA) and mPZRb R2: (CCGGAATTCCGGTCAACTGTGC GTAAATGACTGGGCCCC) for mPZR and mPZRb, respectively. These were PCR amplified from a mouse E17 embryo cDNA library (Clontech Laboratories, Inc.) and inserted into the pIRES-EGFP vector (Clontech Laboratories, Inc.) at the EcoRI restriction site after restriction digestion and ligation using the T4 ligase (Promega Ltd) and sequenced as above. After maxiprep purification using the Qiagen gel extraction kit (Qiagen Ltd), these mPZR-flag-pIRES-EGFP and mPZRb-flag-pIRES-EGFP constructs were transiently transfected independently into NIH3T3 cells using the Lipofectamine 2000 reagent (Gibco-BRL) in a 1:2 ratio, according to the manufacturer's protocol. The expression was determined by flow cytometry using the anti-Flag-epitope Mab, M2, and appropriate isotype matched control Mabs as above.

### In Vitro Migration Assay

NIH3T3 cells ($10^5$ cells/ml) were seeded in DMEM with 10% (v/v) FCS in six-well plates coated with human plasma fibronectin (20 μg/ml; Sigma–Aldrich Ltd) or 1% (w/v) gelatin (Sigma–Aldrich), or alternatively on collagen type IV and laminin coated plates which were purchased from Biocat (Becton-Dickinson). When confluent, a one mm strip of cells was removed from the center of the well with an Eppendorf pipette tip, prior to washing the monolayer and further incubation in DMEM medium with 10% (v/v) FCS. The migration of the cells into the cell-free strip was determined by capturing images of the migrating cells within pre-marked zones on a T-300 Nikon inverted microscope fitted with a Coolpix 900 digital camera (both from Nikon Ltd), immediately after the cell free strip was made and after 6 h incubations at 37°C in a 5% (v/v) humidified $CO_2$ incubator. The area (width of the scratch X diameter ($cm^3$)) of the cell free zone was measured and used to calculate the speed of cell migration over these time points. Experiments were repeated three times each, following independent transfections. Statistical analysis was performed using Student's *t*-Test, where *P*-values $<0.05$ are considered significant.

### Western Blotting and Immunoprecipitation

Protein G Sepharose beads (Amersham-Pharmacia, Amersham, Bucks, UK) were pre-armed with the anti-Flag-epitope Mab, M2, or isotype control Mab and incubated at 4°C with cell lysates from NIH3T3, mPZR-pIRES-EGFP, and mPZRb-pIRES-EGFP transfected and expressing NIH3T3 cells grown on fibronectin. The samples were then subjected to 10% (w/v) SDS–PAGE, transferred to PVDF membranes (Gibco-BRL), blotted with anti-Flag-epitope Mab, M2, or SHP-2 polyclonal antibody (Cell Signaling Technology), and developed with horseradish peroxidase (HRP)-conjugated secondary antibodies (Pierce Biotechnology, Ltd, Tattenhall, Cheshire, UK). Immunoreactive proteins were developed using the ECL system (Amersham-Pharmacia) and exposed to Kodak X-O MAT film (Eastman Kodak, Rochester, NY). The protocol was essentially as detailed in Zannettino et al. [2003].

## RESULTS

### Conservation of Nucleotide and Genomic Structures Between mPZR and hPZR

The mPZR (GeneBank accession number: **AY764247**) and mPZRb (GeneBank accession number: **AY764248**) sequences obtained by PCR amplification of cDNA libraries derived from hematopoietic cell lines, P388D1, MEL-585 and FDCP-mixA4 are shown in Figure 1A,B. These share more than 84% nucleotide identity with the equivalent human PZR isoforms, hPZR, and hPZRb (Fig. 1A,B, respectively). In addition to highly conserved nucleotide sequences, the mPZR gene exhibits a remarkable similarity with the human gene in terms of genomic structure, chromosomal location and exon usage for generating mPZR isoforms. Analysis of the genomic structure revealed that mPZR isoforms, like the equivalent hPZR splice variants, are generated from a single transcription unit on murine chromosome 1 by alternative splicing (Fig. 1C). The genomic sequence of mPZR consists of six exons and five introns, and covers at least 42 kb of DNA on the mouse chromosome 1. The shorter isoform, mPZRb, splices from exon 4 onto exon 6 at position +604, and reads through to a stop codon (TTA) at position +627. A 3′-untranslated region (3′-UTR) of approximately 1 kb can be predicted from the mPZR cDNA sequence

(Fig. 1A,B). Furthermore, intron 1 is the longest intron in both human and mouse genes, being 43.3 and 25.7 kb in length respectively (compare Fig. 1C with Reference Zannettino et al. [2003]). The mouse ortholog of human PZRa, as described in Reference Zannettino et al. [2003], was not detected by PCR analysis. Although, not quantitative, RT-PCR analysis of the multipotent FDCP-mix A4, monocytic P388, T lymphoid EL-4 and erythroid MEL585 hematopoietic cell lines (Fig. 1D) suggested higher levels of mPZR expression when compared to mPZRb in the multipotent and moncytic cell lines, low expression of both isoforms in the T cell line and essentially equivalent levels of expression in the erythroid cell line. The levels of expression of mPZR compared to mPZRb were therefore confirmed using real-time

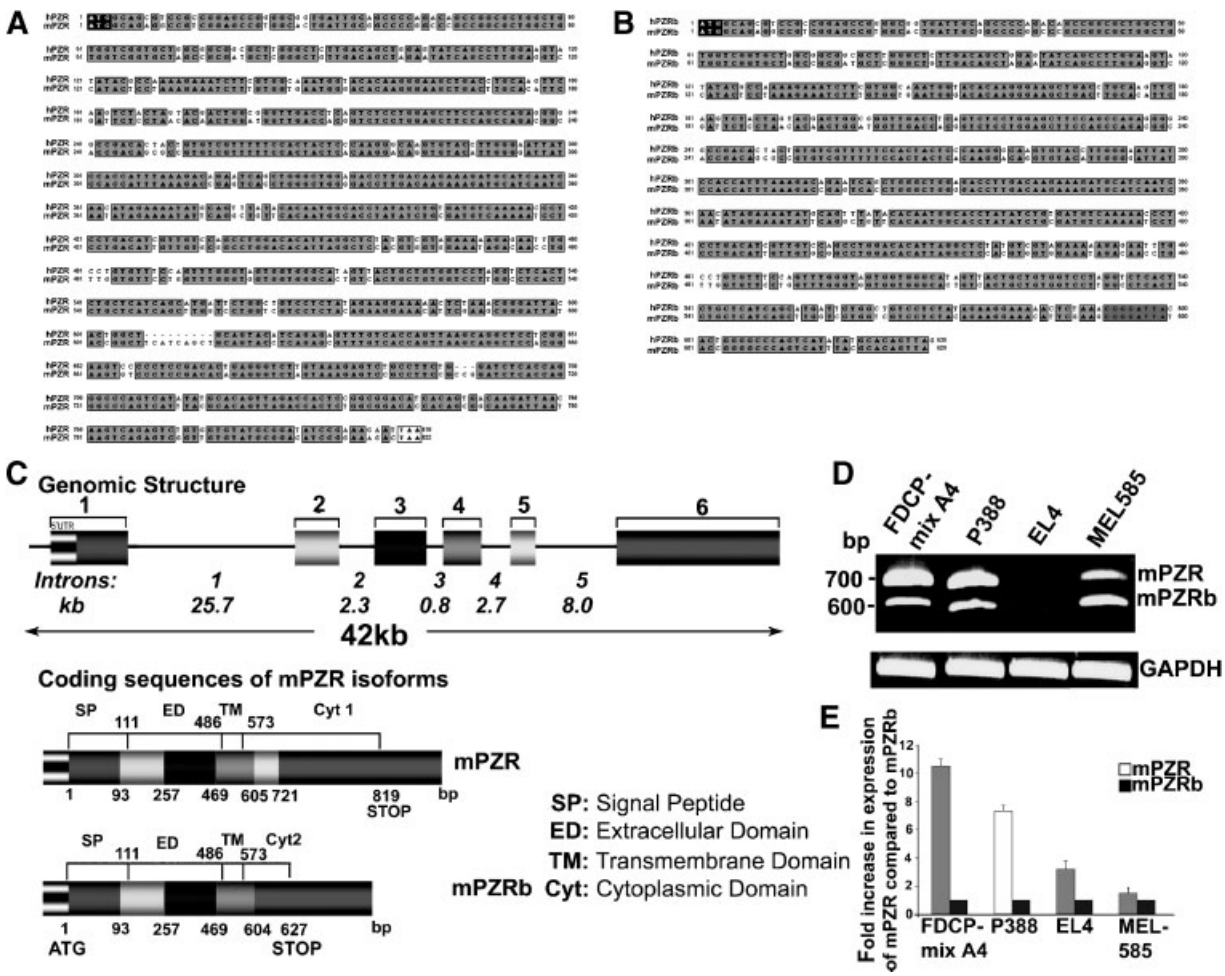


**Fig. 1.** PZR isoforms are highly conserved in the human and mouse. **A**,**B**: Nucleotide sequence comparisons of mPZR and mPZRb with hPZR and hPZRb, respectively. Sequences were aligned using MacVector software. Nucleotide sequence identity is highlighted in the gray boxes. **C**: A schematic representation of the genomic structure of the mPZR gene, showing exons 1–6 (boxes) and, in italics, introns 1–5 (black lines). The mPZR isoform is encoded by exons 1–6, whereas mPZRb lacks exon 5. The similarity to the genomic structure of the hPZR and hPZRb isoforms is shown. Sequences encoding the signal peptide (SP), and the extracellular (ED), transmembrane (TM), and cytoplasmic (Cyt1 and Cyt2) domains are indicated for mPZR and mPZRb. **D**: PCR analyses of cDNA libraries derived from hematopoietic cell lines, P388D1, MEL-585, EL-4 and FDCP-mixA4, using mPZR and mGAPDH primer pairs (see Materials and Methods). The mPZR primer set generated two PCR products of 700 and 600 bp (**upper panel**) that correspond by sequence analysis to mPZR and mPZRb, respectively. Only low levels of the mPZR isoforms were detected in EL-4 cells. **E**: The relative levels of expression of the mPZR isoform to the mPZRb isoform were determined using real-time quantitative PCR after standardizing each against the house-keeping gene GAPDH and normalizing mPZRb levels in each cell line to 1. This revealed $10.5 \pm 0.3$-, $7.3 \pm 0.3$-, and $1.3 \pm 0.4$-fold higher levels of mPZR expression than of mPZRb in FDCP-Mix A4, P388, and MEL-585 cells, respectively. Although the expression of mPZR isoforms was very low in EL-4 cells, mPZR expression exceeded mPZRb expression by $3.2 \pm 0.3$-fold. Results are expressed as means $\pm$ SEM for three independent experiments.

quantitative PCR after normalizing mPZRb levels in each cell line to 1 (Fig. 1E and see Materials and Methods). The mPZR isoform predominated in each of the cell lines tested, but to the greatest extent in the multipotent and monocytic cell lines tested (Fig. 1E).

### Isoforms and Predicted Peptide Structures of mPZR Are Highly Conserved in the Mouse and Human

The amino acid sequences of mPZR and mPZRb predict type 1 transmembrane proteins of 273 and 209 amino acids, respectively (Fig. 2 and Table I). They are identical in their extracellular and transmembrane domains, but differ in their cytoplasmic tails. Both are predicted to contain three potential N-linked glycosylation sites at positions 50, 64 and 130, in contrast to the hPZR isoforms, which contain only two N-linked glycosylation sites at positions 50 and 130. Two conserved cysteine residues, that are predicted to form the intra-disulfide bridges of an Ig fold, are present at positions 59 and 135 in their extracellular regions, exactly at the same positions as found for the human isoforms (Fig. 2A,B). The IgV-set domains of both the human and murine PZR isoforms share 99.1% identity with the Immunoglobulin domain variable (IgV) region subfamily. Overall, the human and murine PZR peptides share 80% amino acid identities and 86% amino acid similarities, with the extracellular domains for both isoforms exhibiting 98% amino acid similarities (Fig. 2A and Table I). The 29 amino acid transmembrane

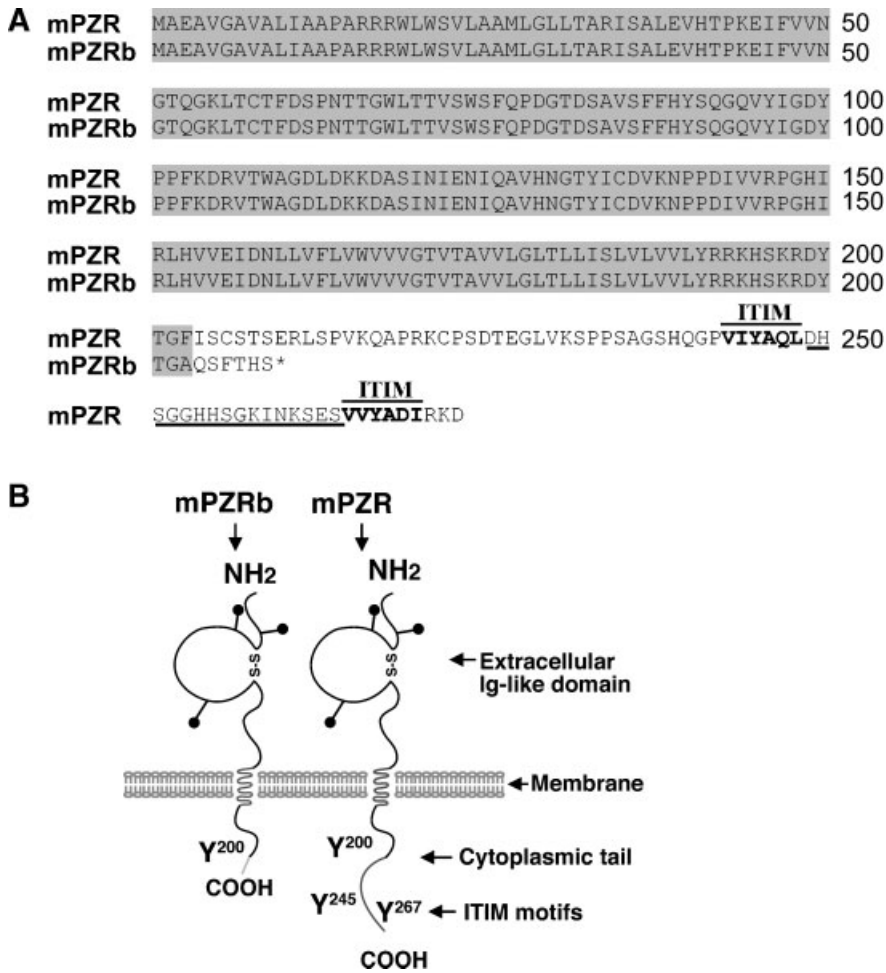


**Fig. 2.** Predicted mPZR and mPZRb peptide sequences and structures and their homologies with other proteins. **A**: Predicted amino acid sequence alignment of mPZR and mPZRb peptides. The identical amino acids are highlighted in grey. The conserved ITIM motifs (bold) and the conserved region between them (underlined) are also indicated. **B**: A schematic representation of mPZR and mPZRb molecules. The predicted phosphotyrosine residues are indicated in the ITIM motifs of mPZR at Y245 and Y267, in addition to predicted N-linked glycosylation sites (—●) and the intrachain disulfide linkage (SS).

**TABLE I. Homology of mPZR Protein[a]**

| mPZR amino acid identities (%) and similarities (%) with | mPZR | | | | | | | |
|---|---|---|---|---|---|---|---|---|
| | Whole peptide | | Extracellular domain | | Transmembrane domain | | Cytoplasmic domain | |
| | Identity | Similarity | Identity | Similarity | Identity | Similarity | Identity | Similarity |
| mPZRb | 76.1 | 76.1 | 100 | 100 | 100 | 100 | 18.8 | 18.8 |
| hPZR | 80.1 | 86.3 | 89.3 | 98.3 | 89.8 | 96.25 | 77.4 | 83.8 |
| m myelin $P_0$ | 52.1 | 45.9 | 41 | 59 | 22.58 | 41.93 | 34.6 | 46.1 |
| m Epithelial V-like antigen | 21.51 | 31.1 | 35.2 | 45.2 | 16.1 | 25.8 | 7.7 | 9.6 |

[a]Homology is demonstrated as percentage of similarity and identity for the whole peptides as well as the sequences representing the extracellular, transmembrane and cytoplasmic domains of mPZRb, hPZR, m myelin $P_0$, and m Epithelial V-like antigen to the mPZR peptide. The MacVector software program was used to determine the similarities and identities.

hydrophobic sequence between amino acids 162 and 191 is followed in mPZR by an 81 amino acid intracellular domain. This contains two classical ITIM motifs (VIY$^{245}$AQL and VVY$^{267}$ADI), with $Tyr_{245}$ and $Tyr_{267}$ being putative phosphorylation sites (Fig. 2A,B). The ITIM motifs and the region between them are conserved in the mouse and human, with the exception of one residue at position 257, where a glutamine residue in mPZR is replaced by an aspartic acid residue in hPZR. The cytoplasmic tail of mPZRb is predicted to be 17 amino acids in length and lacks the two ITIM motifs. This is reminiscent of human PZRb [Zannettino et al., 2003]. Interestingly, and similarly to hPZR, mPZR exhibits its closest amino acid similarities with the murine myelin $P_0$ protein (52% identity and 46% similarity overall) and the murine epithelial-like antigen (21% identity and 31% similarity overall), suggesting that these molecules may have similar or related functions (Table I). Both the human and murine proteins are predicted to have similar structures (compare Fig. 2B with Reference Zannettino et al. [2003]).

### The mPZR Protein Accelerates Cell Motility on Fibronectin

Human PZR has been shown to possess a unique function in that it modulates cell migration on a fibronectin substrate in a SHP-2-dependent manner [Zannettino et al., 2003]. In order to determine if mPZR functions in a similar manner, murine NIH3T3 cells, which exhibit low levels of endogenous mPZR isoforms, were transiently transfected with Flag-tagged mPZR or mPZRb constructs and shown by flow cytometry using an anti-Flag Mab to express these proteins (Fig. 3A,B, respectively). The molecular weights of the Flag-tagged mPZR and mPZRb proteins were identified at approximately 45 and 43 kD, respectively, after immunoprecipitation analysis with the anti-Flag Mab (Fig. 3A,B insets). These mPZR and mPZRb expressing cells were then analyzed for their ability to migrate on fibronectin (Fig. 3C), collagen, laminin or gelatin matrices (Fig. 3D). A fourfold statistically significant ($P < 0.004$) increase in migration on fibronectin only of NIH3T3 cells expressing mPZR was observed when compared with mPZRb or mock-transfected NIH3T3 cells and with other matrices (Fig. 3D). In addition, in the presence of fibronectin, mSHP-2 interacts with the mPZR molecule. This was established by identification of a band of approximately 63 kD, corresponding to mSHP-2, in the presence of mPZR, but not of mPZRb, after co-immunoprecipitation with the anti-Flag Mab and Western blotting with the anti-Flag Mab to detect mPZR and mPZRb (Fig. 3E (a–c)) or the anti-SHP-2 polyclonal antibody (Fig. 3E (d–f)).

### mPZR Is Absent From mES Cells, but Upregulated by Day 3 of Murine Embryoid Body Development In Vitro

PCR analysis revealed that both mPZR isoforms were present in E11 to E17 day murine embryos and in a variety of adult tissues (data not shown). Real-time quantitative PCR analyses showed that the mPZR is more highly expressed than mPZRb in all samples tested whether embryonic or adult (Fig. 4A). This was particularly evident in adult tissues such as the kidney, spleen and lung (Fig. 4A). When the expression levels of mPZR in tissues or embryos were analyzed relative to one another, the murine embryo at E17 expressed higher mPZR levels than was observed at the earlier stages of

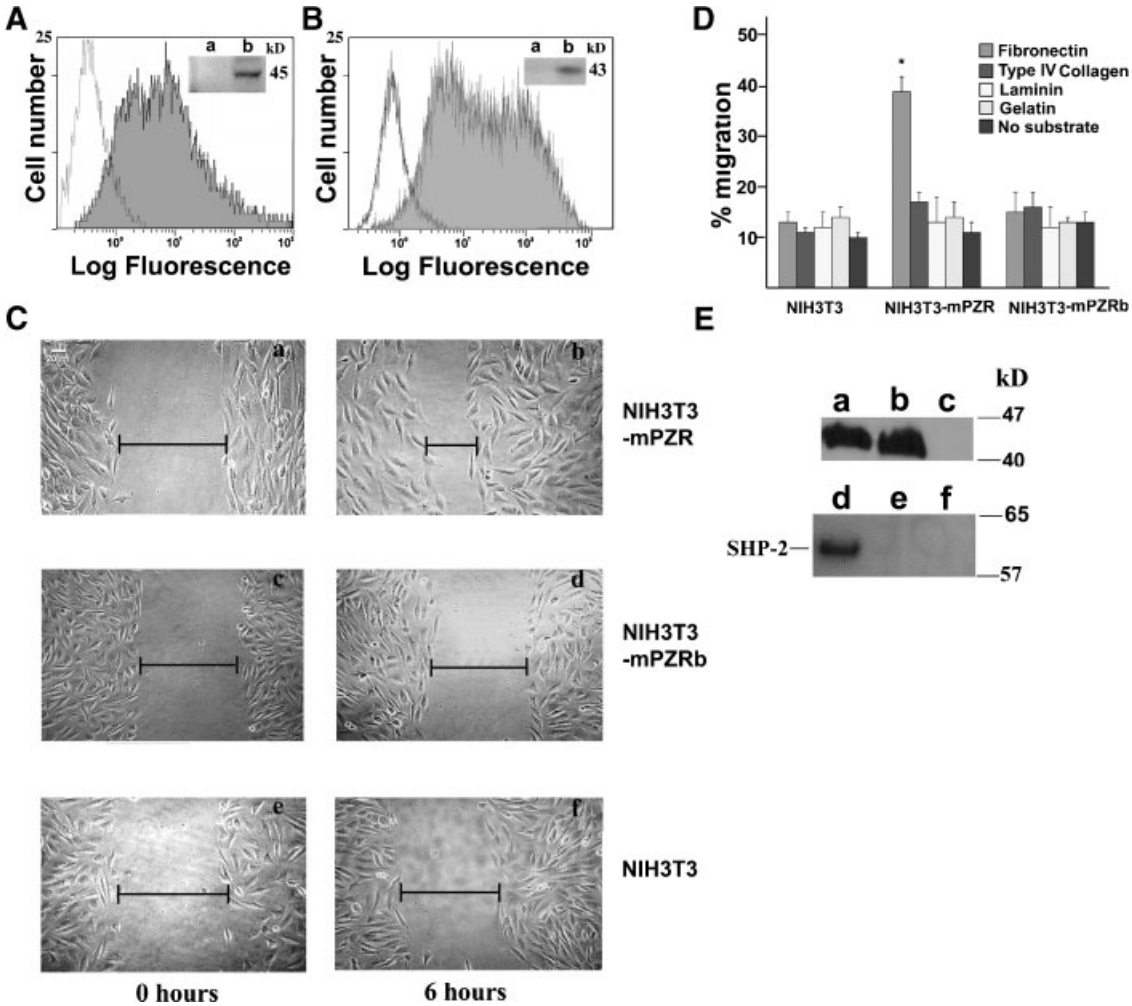


**Fig. 3.** Murine PZR accelerates cell migration on fibronectin. **A**,**B**: Representative single-color flow cytometric analysis showing binding of the anti-Flag Mab, M2, (filled histograms) to NIH3T3 cells overexpressing the flag-tagged mPZR protein (A) and the Flag-tagged mPZRb protein (B), but the lack of binding of the isotype-matched mIgG1 negative control Mab (open histograms). Insets to A,B: Apparent molecular mass of respective mPZR and mPZRb isoforms after flag-mPZR-IRES-EGFP-transfected NIH3T3 cells and flag-mPZRb-IRES-EGFP-transfected NIH3T3 cells were subjected to immunoprecipitation with isotype negative control (a) or anti-Flag M2 (b) Mabs, electrophoresed on a 2.5–12% (w/v) SDS–polyacrylamide gel and blotted with anti-Flag M2 Mab. **C**: The relative migration of mPZR- (a,b), mPZRb- (c,d), or non- (e,f) expressing NIH3T3 cells on fibronectin-coated dishes at time zero (0 h), the commencement time for cell migration, and 6 h after the migration commenced (see Materials and Methods). NIH3T3 cells overexpressing mPZR migrate more rapidly on fibronectin than those expressing mPZRb or non-expressing control cells. **D**: Histograms showing the percentage increase in migration on various matrices of NIH3T3 overexpressing mPZR, compared to mPZRb- or non-expressing NIH3T3 cells. A significant difference ($P < 0.004$, Student's *t*-test) in the migration potential was conferred to cells expressing mPZR migrating on fibronectin compared to cells expressing mPZR and migrating on other matrices. **E**: The (a,d) flag-mPZR-, (b,e) flag-mPZRb-, or (c,f) non-expressing NIH3T3 cells were cultured on fibronectin-coated plates and then immunoprecipitated with anti-Flag M2 Mab, electrophoresed on a 2.5–12% (w/v) SDS–polyacrylamide gel and blotted with anti-Flag M2 Mab (a,b,c) or with rabbit polyclonal anti-SHP-2 antibody (d,e,f).

murine embryonic development or in adult tissues tested (Fig. 4B). In the latter, the testis had the highest level of expression of those adult tissues tested (Fig. 4B).

Since mPZR and mPZRb are also expressed in the primitive multipotent hematopoietic stem cell line, FDCP-mix A4 (Fig. 1D,E and data not shown), and since mSHP-2 is present in self-renewing mES cells (Fig. 4D), we hypothesized that mES cells might also express the mPZR isoforms. Our studies, however, revealed that both isoforms were absent from self-renewing, undifferentiated mES cells (Fig. 4C,D). We therefore exploited the mES/EB in vitro model system in order to determine the time of appearance of mPZR isoforms during the early

stages of murine embryogenesis. The differentiation of mES cells into EBs in vitro was followed daily for 6 days (Fig. 4C). The pluripotency of mES cells was determined by expression of mOCT-4, the differentiation of mES cells to early mesoderm and ventral mesoderm by expression of mBRACHYURY and mBMP-4 respectively, and the commitment of ES cells to hematopoietic and endothelial lineages at the hemangioblast stage and their subsequent lineage development by expression of mBMP-4 and then mFLK-1. The mPZR and mPZRb isoforms were upregulated by day 3 of EB differentiation (Fig. 4D), appearing after the expression of mOCT-4 and mBRACHYURY transcripts. mPZR isoform expression coincided with weak, but detectable levels, of mBMP-4 transcripts, but preceded the upregulation of mFLK-1 by approximately 1 day (Fig. 4D). Analysis of the expression of the mPZR docking molecule, mSHP-2, revealed that even though it was expressed in undifferentiated mES cells, its expression was maintained during differentiation of these cells into EBs over the 6 day period examined and during the upregulation of the mPZR isoforms (Fig. 4D).

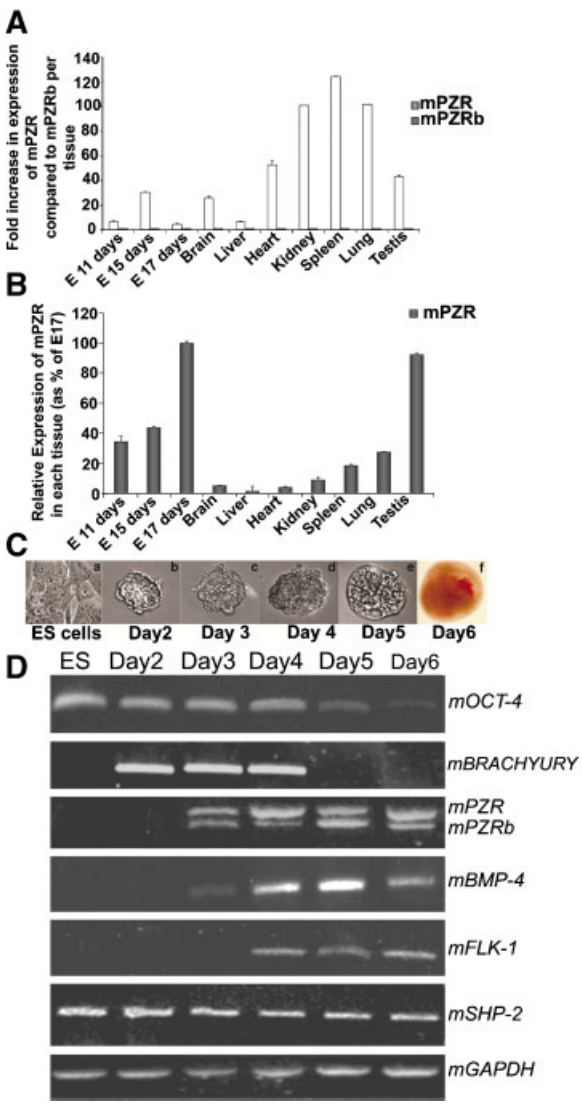


**Fig. 4.** The mPZR splice variants are not expressed in self-renewing mES cells, but are upregulated during embryonic development. **A**: Real-time quantitative PCR analysis comparing the relative expression of mPZR to mPZRb in different tissues, after standarization against GAPDH and after mPZRb was normalized to 1 for each tissue. A cDNA panel of murine embryos at differing stages of development and of adult tissues was used in the analyses. Results are expressed as means ± SEM for three independent experiments. All samples tested showed higher levels of mPZR expression. Sequence analyses of 700 and 600 bp of RT-PCR products corresponding to mPZR and mPZRb respectively confirmed their presence in all these tissues. **B**: Real-time quantitative PCR analysis comparing the relative expression of mPZR in different murine embryonic (day E11 to E17) and adult tissues after standardization against GAPDH. The most highly expressing sample, E17, was normalized to 100% and the relative levels of mPZR expression calculated as a percentage of this value. **C**: Murine ES cells were differentiated in vitro to embryoid bodies (EBs) over 6 days and images captured daily on a Nikon T-300 microscope at 10× and 40× magnification. On day 6, hematopoietic development can be easily visualized by the red color of the EB. **D**: RT-PCR analyses of genes that specifically mark pluripotent murine ES cells (mOCT-4) and their mesodermal differentiation (mBRACHYURY, mBMP-4, mFLK-1) during EB formation in vitro were carried out daily for 6 days of EB differentiation in parallel to those for mSHP-2, mPZR, and mPZRb. The mGAPDH gene was used as a positive control at all timepoints. Primer sets designed to amplify mOCT-4, mBRACHYURY, mBMP-4, mFLK-1, mPZR, mPZRb, mSHP-2 and mGAPDH are described in Materials and Methods. [Color figure can be viewed in the online issue, which is available at www.interscience.wiley.com.]

### mPZR Protein Is Expressed in the Blastocyst and the Developing Embryo In Vivo

To confirm the in vitro mES/EB expression analysis results described above, we recovered day E1.5 (24 h post-hCG, two cell stage) and E3.5 (96 h post-hCG, blastocyst stage) embryos from pregnant mice for in situ immunofluorescent analysis. Considering the extremely high amino acid similarity between the extracellular domains of human and mouse PZR isoforms, we tested by flow cytometry whether the WM78 Mab would cross-react with the mouse PZR isoforms expressed by the PZR isoform positive mouse cell line, MEL-585 or with NIH3T3 flag-mPZR-IRES-EGFP and NIH3T3 flag-mPZRb-IRES-EGFP transfected cells. Figure 5A,B demonstrate that the WM78 Mab binds to both

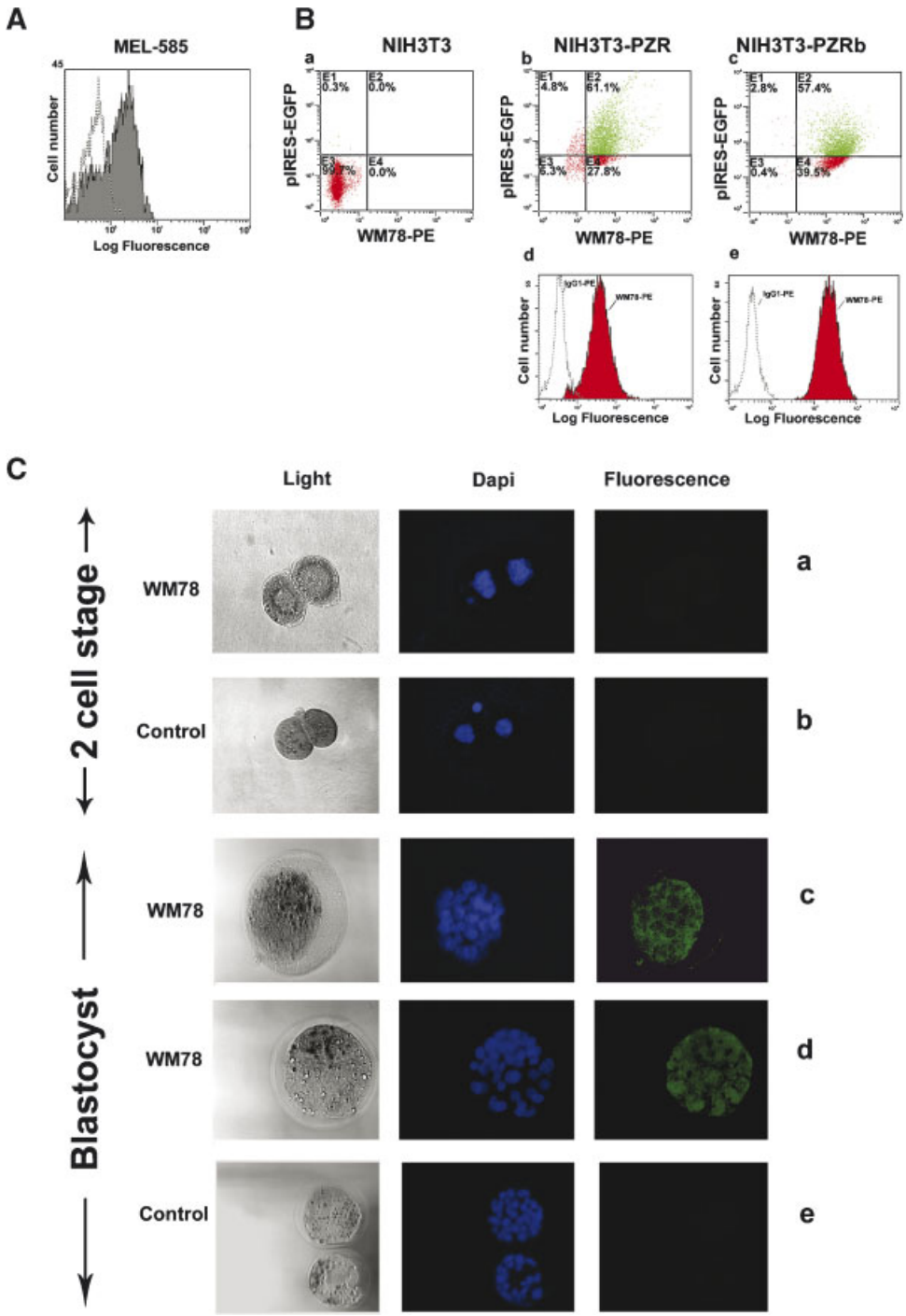


**Fig. 5.** The mPZR splice variants are upregulated during embryogenesis. **A**: FACS analysis demonstrating that WM78 Mab (filled histogram) reacts with the mPZR isoforms in MEL-585 cells. The unfilled histogram represents the isotype matched negative control. A secondary goat anti-mouse FITC-conjugated antibody was used to detect fluorescence. **B**: FACS dotplots demonstrating that WM78 Mab (detected with rabbit anti- mouse PE-conjugated antibody) can specifically react with the mPZR isoforms in flag-mPZR-IRES-EGFP-transfected NIH3T3 cells (b,d) and in flag-mPZRb-IRES-EGFP-transfected NIH3T3 cells (c,e), respectively, in contrast to sham transduced NIH3T3 cells (a) where no binding was identified. The ordinate shows the fluoresecence of cells expressing EGFP. There was lack of binding of the isotype-matched mIgG1 negative control Mab (open histograms; d,e) compared with positive binding with WM78 Mab (filled histograms; d,e). **C**: The WM78 Mab was used for in situ immunofluorescent staining of murine embryos at days E1.5 and E3.5 (c,d) and the reaction developed with an Alexa-488 goat anti-mouse IgG1 secondary antibody. The Alexa-488 goat anti-mouse IgG1 secondary antibody was used as negative control for embryos of the same time points (days E1.5 (b) and E3.5 (e)), respectively. [Color figure can be viewed in the online issue, which is available at www.interscience.wiley.com.]

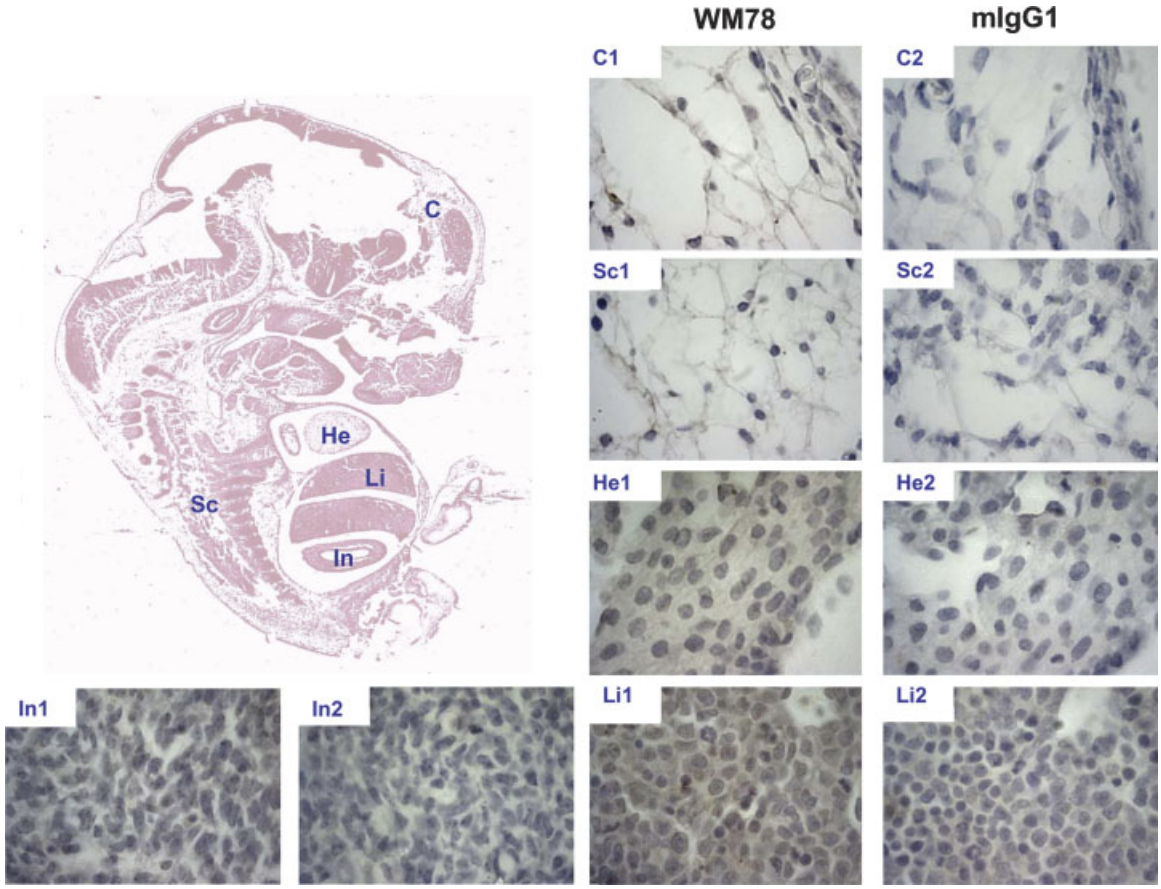


**Fig. 6.** The mPZR splice variants are expressed in various tissues during murine embryonic development. The WM78 Mab was used for in situ immunocytochemical staining of murine day E12.5 embryo sections (**upper left** figure) and staining developed with biotinylated anti-mouse IgG secondary antibody and streptavidin-peroxidase (C1, Sc1, He1, Li1, In1). An anti-mouse IgG1 primary antibody was used as negative control for staining (C2, Sc2, He2, Li2, In2). The sections presented are cranial parenchyma (C), spinal cord tissues (Sc), heart (He), liver (Li), and intestine (In). [Color figure can be viewed in the online issue, which is available at www.interscience.wiley.com.]

the MEL-585 cells (Fig. 5A) and to the NIH3T3 cells expressing mPZR (Fig. 5B (b,d)) or mPZRb (Fig. 5B (c,e)) in contrast to sham transfected NIH3T3 cells where no significant binding was detected (Fig. 5B (a)). Using the WM78 Mab, we could not detect the mPZR isoforms at day E1.5 of embryogenesis (Fig. 5C (a)) but these were evident by day E3.5 (Fig. 5C (c,d)), where staining appeared ubiquitous. Negative controls from each time point are presented in Figure 5C (b,e). By day E12.5 of embryonic development, weak but positive staining with the WM78 Mab was evident in the following tissues: the cranial parenchyma (Fig. 6(C1)), spinal cord (Fig. 6 (Sc1)), heart (Fig. 6 (He1)), and lung (data not shown). It was notable that the fetal liver, a major hematopoietic organ during fetal development, showed stronger staining (Fig. 6 Li (1)), while the intestine (Fig. 6 In (1)) did not stain with the WM78 Mab.

## DISCUSSION

In this article, we have identified and cloned the ITIM-containing murine ortholog of hPZR, mPZR, and its ITIM-less isoform, mPZRb. Importantly, we have demonstrated that mPZR mimicks hPZR [Zannettino et al., 2003] structurally, and also functionally, by its ability to bind to mSHP-2 and to increase cell migration on fibronectin. Notably, the ITIM-less mPZRb isoform does not bind mSHP-2 nor enhance cell migration. The mPZR gene, like its human counterpart, is located on the long arm of chromosome 1 and shares its closest homology with myelin $P_0$ protein. While natural mutations in the latter lead to neuropathies, such as

Charot-Marie-Tooth disease and Dejerne-Sottas syndrome in the human [Xu et al., 2000, 2001; Legius et al., 2002; Runker et al., 2004], neither those in hPZR nor in mPZR have been described, although upregulation of hPZR has been recently reported in schizophrenia brain tissue [He et al., 2006]. It is of interest that deficiency of or mutation in the hPZR binding partner, hSHP-2, gives rise to skeletal, vascular, and hematopoietic malformations that can result in Noonan and Leopard syndromes, cardiovascular diseases and myeloid leukemias [Araki et al., 2004; Tartaglia et al., 2004].

Murine ES cells have become crucial and powerful tools for studying gene expression during mammalian development, being capable of generating murine tissues derived from endoderm, mesoderm or ectoderm [reviewed by Keller, 2007]. We have examined, for the first time, the expression patterns of the mPZR and mPZRb isoforms in the earliest totipotent mES cells and during their subsequent early development into EBs in vitro, comparing them with mSHP-2 and genes characteristic of hematopoietic/endothelial development. During the initial stages of differentiation, EB formation recapitulates the temporal pattern of gene expression in the early embryo by the downregulation of the pluripotency gene, mOCT-4, and the upregulation first of the mBRACHYURY transcription factor (an early mesodermal marker), then of mBMP-4 and mFLK-1. In the murine embryo and in differentiating EBs, mBRACHYURY, and mFLK-1 are both expressed by a transient mesodermal subset that undergoes commitment to hematopoietic and endothelial cells and that may represent the common hemangioblast progenitor [reviewed by Keller, 2007]. mBMP-4 mediated signals are required for the induction of mFLK-$1^+$ cells, while VEGF, a FLK-1 ligand, is required for the expansion, movement or differentiation of the Scl/tal-1 expressing endothelial and haematopoietic progenitor cells within the FLK-$1^+$ cell subset [reviewed by Baron, 2003; Park et al., 2004; Keller, 2007]. In our studies, mPZR isoforms were notably absent from undifferentiated, self-renewing mES cells. The expression of both mPZR isoforms was preceded by the expression of mBRACHYURY, and appeared first by day 3 of EB-induced differentiation, as mBMP-4 became expressed. They continued to be expressed as both mBMP-4 and mFLK-1 were upregulated. This indicates that mPZR isoforms do not function in mES cell self-renewal, and that their expression may precede or co-incide with the development of the hemangioblast in vitro.

As an initial step in analyzing the in vivo role of the PZR isoforms in normal development, we have demonstrated the expression of mPZR isoforms by in situ immunofluorescent analysis in recovered mouse embryos. At embryonic day E3.5 in vivo, the developing murine embryo comprises the inner cell mass, which gives rise to the embryo itself and the extra-embryonic membranes, and the trophoectoderm, which contributes to the trophoblast layers of the placenta [Rossant, 2001]. Our analyses demonstrate that mPZR isoforms are ubiquitously expressed at this early blastocyst stage of development, but not at day E1.5. By day E12.5 of embryogenesis, mPZR isoforms were found to be weakly expressed in the spinal cord, cranial parenchyma, heart, and the lung, and more highly in the fetal liver, a major site of definitive hematopoiesis in the embryo. This, together with the relatively high levels of expression of mPZR isoforms in multipotent hematopoietic and myeloid cell lines, may be indicative of an important role in myelopoiesis.

In contrast to mPZR isoform expression, our studies, which confirmed those of Chan et al. [2003], show that mSHP-2 is expressed in self-renewing mES cells and is then maintained throughout the stages of EB formation studied here. It, thus, precedes the expression of, but is subsequently co-expressed with, its binding partner, mPZR. Interestingly, mSHP-2 gene expression has been shown to be critical for mES cell differentiation [Chan et al., 2003; Yang et al., 2006], since a lack of normal mSHP-2 in mES cells expressing a SHP-2 catalytically inactive mutant SHP-$2\Delta^{46-116}$ results in decreased differentiation to/of hemangioblasts. This does not, however, exclude an additional role in cell migration in the embryo, a process crucial for morphogenesis. Indeed, both SHP-2 and PZR have important functions in integrin-mediated cell motility [Oh et al., 1999; Saxton and Pawson, 1999; Yu et al., 2000; Zannettino et al., 2003; Roubelakis and Watt, unpublished data], and, as with the hematopoietic system [Hirsch et al., 1996], integrins play a role in cell formation and/or movement in the developing embryo [Yang et al., 1993; reviewed by O'Shea, 2004] and are required for early vasculogenesis and angiogenesis during embryo formation

[Francis et al., 2002]. Since we have shown that mPZR appears at the earliest stage of EB formation and can bind to mSHP-2 by virtue of its ITIM containing cytoplasmic domain, we hypothesize that mPZR may modulate SHP-2 activity by reducing integrin-mediated adhesion and promoting migration of the developing hemangioblast or its progeny. A subsequent increase in expression of mPZRb during development may modulate this activity of mPZR.

These studies therefore provide the basis for future gene targeting/knockdown experiments to confirm these predicted and other roles of the mPZR isoforms, and to define interacting partners and their functional role in vivo as regulators of cell migration.

## ACKNOWLEDGMENTS

This research is supported by the Leukaemia Research Fund (MR, SMW), Medical Research Council and NHS Blood and Transplant Authority (MR, EM-R, GT, SMW). We would like to thank Professors M. Contreras and D. Anstee for their support, Dr. Catherine Porcher for the mES cell line and for advice on EB cell differentiation, and Dr. Andrew Zannettino for the WM78 Mab. We would also like to thank Dr. Sideras for providing us with the animal models and Dr. Pagakis for advice on confocal images. The research was carried out at the National Blood Service Oxford Centre and benefits from R&D funding received from the NHS R&D Directorate.

## REFERENCES

Araki T, Mohi MG, Ismat FA, Bronson RT, Williams IR, Kutok JL, Yang W, Pao LI, Gilliland DG, Epstein JA, Neel BG. 2004. Mouse model of Noonan syndrome reveals cell type- and gene dosage-dependent effects of Ptpn11 mutation. Nat Med 10:849–857.

Baron MH. 2003. Embryonic origins of mammalian hematopoiesis. Exp Hematol 31:1160–1169.

Burdon T, Smith A, Savatier P. 2002. Signalling, cell cycle and pluripotency in embryonic stem cells. Trends Cell Biol 12:432.

Chan JY, Prudhoe JE, Jorgensen B, Doyonnas R, Zannettino ACW, Buckle VJ, Ward CJ, Simmons PJ, Watt SM. 2001. Relationship between novel isoforms, functionally important domains, and subcellular distribution of novel CD164/endolyn. J Biol Chem 276:2139–2152.

Chan RJ, Johnson SA, Li Y, Yoder MC, Feng GS. 2003. A definitive role of Shp-2 tyrosine phosphatase in mediating embryonic stem cell differentiation and hematopoiesis. Blood 102:2074–2080.

Francis SE, Goh KL, Hodivala-Dilke K, Bader BL, Stark M, Davidson D, Hynes RO. 2002. Central roles of alpha5-beta1 integrin and fibronectin in vascular development in mouse embryos and embryoid bodies. Arterioscler Thromb Vasc Biol 22:927–933.

He G, Liu X, Qin W, Chen Q, Wang X, Yang Y, Zhou J, Xu Y, Gu N, Feng G, Sang H, Sang H, Wang P, He L. 2006. MPZL1/PZR, a novel candidate predisposing schizophrenia in Han chinese. Mol Psychiatry 11:748–751.

Heyworth CM, Alauldin M, Cross MA, Fairbairn LJ, Dexter TM, Whetton AD. 1995. Erythroid development of the FDCP-Mix A4 multipotent cell line is governed by the relative concentrations of erythropoietin and interleukin 3. Br J Haematol 91:15–22.

Hirsch E, Iglesias A, Potocnik AJ, Hartmann U, Fassler R. 1996. Impaired migration but not differentiation of haematopoietic stem cells in the absence of beta1 integrins. Nature 380:171–175.

Keller GM. 1995. In vitro differentiation of embryonic stem cells. Curr Opin Cell Biol 7:862–869.

Keller GM. 2007. Embryonic stem cell differentiation: emergence of a new era in biology and medicine. Genes Dev 19:1129–1155.

Keller G, Kennedy M, Papayannopoulou T, Wiles MV. 1993. Hematopoietic commitment during embryonic stem cell differentiation in culture. Mol Cell Biol 13: 473–486.

Keller G, Lacaud G, Robertson S. 1999. Development of the hematopoietic system in the mouse. Exp Hematol 27: 777–787.

Legius E, Schrander-Stumpel C, Schollen E, Pulles-Heintzberger C, Gewillig M, Fryns JP. 2002. PTPN11 mutations in LEOPARD syndrome. J Med Genet 39:571–574.

Neel BG, Gu H, Pao L. 2003. The 'Shp'ing news: SH2 domain-containing tyrosine phosphatases in cell signaling. Trends Biochem Sci 28:284–293.

Oh ES, Gu H, Saxton TM, Timms JF, Hausdorff S, Frevert EU, Kahn BB, Pawson T, Neel BG, Thomas SM. 1999. Regulation of early events in integrin signaling by protein tyrosine phosphatase SHP-2. Mol Cell Biol 19: 3205–3215.

O'Shea KS. 2004. Self-renewal vs. differentiation of mouse embryonic stem cells. Biol Reprod 71:1755–1765.

Park C, Afrikanova I, Chung YS, Zhang WJ, Arentson E, Fong Gh G, Rosendahl A, Choi K. 2004. A hierarchical order of factors in the generation of FLK1- and SCL-expressing hematopoietic and endothelial progenitors from embryonic stem cells. Development 131:2749–2762.

Qu CK, Yu WM, Azzarelli B, Cooper S, Broxmeyer HE, Feng GS. 1998. Biased suppression of hematopoiesis and multiple developmental defects in chimeric mice containing Shp-2 mutant cells. Mol Cell Biol 18:6075–6082.

Rossant J. 2001. Stem cells from the Mammalian blastocyst. Stem Cells 19:477–482.

Runker AE, Kobsar I, Fink T, Loers G, Tilling T, Putthoff P, Wessig C, Martini R, Schachner M. 2004. Pathology of a mouse mutation in peripheral myelin protein P0 is characteristic of a severe and early onset form of human Charcot-Marie-Tooth type 1B disorder. J Cell Biol 165: 565–573.

Saxton TM, Pawson T. 1999. Morphogenetic movements at gastrulation require the SH2 tyrosine phosphatase Shp2. Proc Natl Acad Sci USA 96:3790–3795.

Saxton TM, Henkemeyer M, Gasca S, Shen R, Rossi DJ, Shalaby F, Feng GS, Pawson T. 1997. Abnormal mesoderm patterning in mouse embryos mutant for the SH2 tyrosine phosphatase Shp-2. EMBO J 16:2352–2364.

Tartaglia M, Mehler EL, Goldberg R, Zampino G, Brunner HG, Kremer H, van der Burgt I, Crosby AH, Ion A, Jeffery S, Kalidas K, Patton MA, Kucherlapati RS, Gelb BD. 2001. Mutations in PTPN11, encoding the protein tyrosine phosphatase SHP-2, cause Noonan syndrome. Nat Genet 29:465–468.

Tartaglia M, Niemeyer CM, Shannon KM, Loh ML. 2004. SHP-2 and myeloid malignancies. Curr Opin Hematol 11:44–50.

Watt SM, Bulter L, Tavian M, Burhing H-J, Rapppold I, Simmons PJ, Zannettino ACW, Buck D, Fuchs A, Doyonnas R, Chan JY-H, Levesque J-P, Peault B, Roxanis I. 2000. Functionally defined CD164 epitopes are expressed on CD34+ cells throughoutonogeny but display distinct distribution patterns in adult hematopoietic and nonhematopoietic tissues. Blood 95:3113–3124.

Xu M, Zhao R, Sui X, Xu F, Zhao ZJ. 2000. Tyrosine phosphorylation of myelin P(0) and its implication in signal transduction. Biochem Biophys Res Commun 267: 820–825.

Xu W, Shy M, Kamholz J, Elferink L, Xu G, Lilien J, Balsamo J. 2001. Mutations in the cytoplasmic domain of P0 reveal a role for PKC- mediated phosphorylation in adhesion and myelination. J Cell Biol 155:439–446.

Yang JT, Rayburn H, Hynes RO. 1993. Embryonic mesodermal defects in alpha 5 integrin-deficient mice. Development 119:1093–1105.

Yang W, Klaman LD, Chen B, Araki T, Harada H, Thomas SM, George EL, Neel BG. 2006. An Shp2/SFK/Ras/Erk signaling pathway controls trophoblast stem cell survival. Dev Cell 10:317–327.

Yu C, Jin Y, Burakoff S. 2000. Cytosolic Tyrosine dephosphorylation of ST AT5.Potential role of SHP-2 in STAT-5 regulation. J Biol Chem 275:599–604.

Zannettino AC, Roubelakis M, Welldon KJ, Jackson DE, Simmons PJ, Bendall LJ, Henniker A, Harrison KL, Niutta S, Bradstock KF, Watt SM. 2003. Novel mesenchymal and haematopoietic cell isoforms of the SHP-2 docking receptor, PZR: Identification, molecular cloning and effects on cell migration. Biochem J 370:537–549.

Zhao R, Zhao ZJ. 2000. Dissecting the interaction of SHP-2 with PZR, an immunoglobulin family protein containing immunoreceptor tyrosine-based inhibitory motifs. J Biol Chem 275:5453–5459.

Zhao R, Guerrah A, Tang H, Zhao ZJ. 2002. Cell surface glycoprotein PZR is a major mediator of concanavalin A-induced cell signaling. J Biol Chem 277:7882–7888.

Zhao R, Fu X, Teng L, Li Q, Zhao ZJ. 2003. Blocking the function of tyrosine phosphatase SHP-2 by targeting its Src homology 2 domains. J Biol Chem 278:42893–42898.